Am J Nucl Med Mol Imaging 2012;2(3):260-270
www.ajnmmi.us /ISSN:2160-8407/ajnmmi1205002

Original Article

[^{125}I]FIAU imaging in a preclinical model of lung infection: quantification of bacterial load

Mrudula Pullambhatla[1], Jean Tessier[2], Graham Beck[3], Bruno Jedynak[3], Jens U Wurthner[2], Martin G Pomper[1]

[1]Russell H. Morgan Department of Radiology and Radiological Sciences, Johns Hopkins University; [2]AstraZeneca Discovery Medicine, Macclesfield, U.K.; [3]Department of Applied Mathematics and Statistics, Johns Hopkins University, Baltimore, Maryland, U.S.A.

Received May 9, 2012; accepted June 11, 2012; Epub July 10, 2012; Published July 30, 2012

Abstract: 2'-Fluoro-2'-deoxy-1β-D-arabinofuranosyl-5-[^{125}I]iodouracil ([^{125}I]FIAU), a substrate for the thymidine kinase (TK) present in most bacteria, has been used as an imaging agent for single photon emission computed tomography (SPECT) in an experimental model of lung infection. Using SPECT-CT we show that [^{125}I]FIAU is specific for bacterial infection rather than sterile inflammation. We report [^{125}I]FIAU lung uptake values of 1.26 ± 0.20 percent injected dose per gram (%ID/g) in normal controls, 1.69 ± 0.32 %ID/g in lung inflammation and up to 7.14 ± 1.09 %ID/g in lung infection in *ex vivo* biodistribution studies at 24 h after intranasal administration of bacteria. Images of [^{125}I]FIAU signal within lung can be used to estimate the number of bacteria present, with a limit of detection of 10^9 colony forming units per mL on the X-SPECT scanner. [^{125}I]FIAU-Based bacterial imaging may be useful in preclinical models to facilitate the development of new antibiotics, particularly in cases where a corresponding human trial is planned.

Keywords: Inflammation, thymidine kinase, nucleoside, SPECT, PET, molecular imaging

Introduction

Bacterial infections are a major cause of morbidity and mortality. The emergence of new pathogens and more importantly, of known pathogens with increased resistance to antibiotics, such as methicillin-resistant *Staphylococcus aureus* (MRSA) [1] and enhanced-spectrum beta-lactamase producing *enterobacteriaceae* (ESBL) [2], have led to an increased awareness of infectious diseases. Patients are prone to developing infections related to immune suppression encountered with cytotoxic anti-cancer chemotherapies [3], following organ transplantation [4] or upon implantation of foreign materials, such as in surgery for a prosthetic joint [5]. Nosocomial infections, in particular, remain a serious if not increasing threat. Diagnosis and therapeutic monitoring of infectious diseases are a constant challenge. Conventional methods of diagnosis rely on blood cultures and/or direct biopsy. Those methods are invasive, time-consuming, subject to sampling error and are not appropriate for all organ systems, e.g., the brain and central nervous system. Imaging provides a noninvasive means of identifying and quantifying infection, but current methods are either nonspecific, such as magnetic resonance imaging or positron emission tomography (PET) with [^{18}F]fluorodeoxyglucose [6, 7], or are cumbersome and insensitive in certain cases, such as the current clinical standard, the tagged white-blood cell scan [8-11]. Newer methods to detect and follow infection involve agents that bind specifically to bacterial proteins, such as the use of radiolabeled analogs of ciprofloxacin [12] and other antibiotics [13] or of radiolabeled chemotactic peptides [14]. Radiopharmaceutical-based methods to image infection have been summarized in several recent reviews [15-17]. One promising new technique uses radiolabeled nucleoside analogs such as 2'-fluoro-2'-deoxy-1β-D-arabinofuranosyl-5-[$^{124/5}$I]iodouracil ([$^{124/5}$I]FIAU) [18-20] or 2'-[^{18}F]fluoro-2'-deoxy-1β-D-arabinofuranosyl-5-ethyluracil ([^{18}F]FEAU) [21], which are substrates of bacterial – but not human – thymidine kinase (TK). The feasibility of using

radiotracers of this class to detect localized bacterial infections in experimental models of infection [18] and in human subjects has been demonstrated [19]. We have also recently used a strain of *M. tuberculosis*, engineered to express TK, which it does not naturally express, to image this infection in mice to provide a noninvasive means to test new antituberculosis agents *in vivo* [20].

Here we report the use of [125I]FIAU to image murine pulmonary bacterial infections. We use this model system to validate the technique, i.e., prove that [125I]FIAU is sequestered only within infected tissue and not in sterile inflammation. We also attempt to quantify the bacterial load through imaging and use the method to follow a brief course of antibiotic treatment.

Materials and methods

Materials

Lipopolysaccharide (LPS) from *Escherichia coli* (serotype 026:B6) was purchased from Sigma (St. Louis, MO). *E. coli* strain RS218 was a kind gift of Dr. Kwang Sik Kim (Johns Hopkins). *E. coli* strain KY895 was obtained from the Coli Genetic Stock Center (CGSC) of Yale University. 2'-Fluoro-2'-deoxy-1β-D-arabinofuranosyl-uracil (FAU) was purchased from ABX Biochemicals (Radeberg, Germany). All other reagents were obtained from Sigma or Fisher Scientific (Pittsburgh, PA).

Animals

All studies were performed in accordance with the regulations of the Johns Hopkins Animal Care and Use Committee. Eight- to 10-week-old CD-1 mice were purchased from Charles River Labs (Wilmington, MA).

[125I]FIAU preparation

The synthesis of [125I]FIAU was performed according to Jacobs et al [22]. Briefly, FAU (300 μg, 1.22 mmol, Moravek) was dissolved in 170 μL of 2 M HNO_3. To that solution, 1.5 mCi (55.5 MBq) of [125I]NaI (ICN Pharmaceuticals, Costa Mesa, CA) was added and the contents were heated at 130°C for 45 min. The reaction was quenched with 150 μL of high-performance liquid chromatography (HPLC) mobile phase (20:79.9:0.1% MeCN: H_2O: triethylamine). The resulting [125I]FIAU was purified by reverse-phase HPLC over a Phenomenex Luna C_{18} semi-prep column (10 μm, 4.6 × 250 mm, Phenomenex, Torrance, CA) by using the isocratic mobile phase mentioned above at a flow rate of 2 mL/min. The product was concentrated under reduced pressure and formulated in 0.9% physiological saline before sterile filtration through a 0.22 μm syringe filter. Formulations were kept at 1 mCi/100μl. (37 MBq/mL) to minimize the injection volume. The final radiochemical yield was ~ 50%, the radiochemical purity was > 99%, and the specific radioactivity was > 74 TBq/mmol.

Lipopolysaccharide (LPS) induced lung inflammation

Mice were anesthetized by brief isoflurane administration. While anesthetized, intranasal instillation was conducted by placing 10 μg/60 μL (167 μg/mL) of LPS onto the nares. The 60 μL sample was applied onto the nares as three 20 μL drops [23, 24]. One mouse per time point was also administered phosphate-buffered saline (PBS) in a similar fashion and was used as the control.

Lung lavage and total cell count

After intranasal exposure to LPS and PBS, mice (n = 4) were sacrificed by cervical dislocation at various time points (0, 12 h, 24 h, 36 h and 48 h). Bronchoalveolar lavage (BAL) was performed as described previously [24]. The total number of cells in the pooled samples was then counted using a hemocytometer.

SPECT-CT imaging of lung inflammation

Eight healthy (8 – 10-week-old) female CD-1 mice (Charles River, Wilmington, MA) were imaged. For the baseline scan all eight animals were injected intravenously with 1 mCi (37 MBq) of radiopharmaceutical. At 2 h post-injection, each mouse was anesthetized with isoflurane and maintained under 1 – 2% isoflurane in oxygen. The mouse was positioned on the X-SPECT (Gamma Medica-Ideas, Northridge, CA) gantry and was scanned using two low energy, high-resolution pinhole collimators (pinhole diameter 10mm) rotating through 360° for 40 sec per increment (total acquisition time ~ 45 minutes). All gamma images were reconstructed using LumaGEM software (Gamma

Medica-Ideas). Immediately following image acquisition, the mice were then scanned by CT (X-SPECT) over a 3.5 cm field-of-view using a 600 μA, 50 kV beam. Data were reconstructed using the Ordered Subsets-Expectation Maximization (OS-EM) algorithm. The SPECT and CT data were then co-registered using the supplier's software (Gamma Medica-Ideas) and displayed using Amira (Visage Imaging Inc., Andover, MA). Immediately following imaging, four mice were administered 60 μL LPS intranasally as described earlier. The remaining four mice were administered 60 μL of PBS (controls) in a similar manner. At 22 h after LPS and PBS administration, each mouse was injected intravenously with 1 mCi (37 MBq) of [125I]FIAU. The injections of radiotracer were staggered to accommodate imaging of every mouse 2 h after injection of radiotracer and coinciding with the 24 h time point after the intranasal administration of LPS or PBS, the time point at which the pulmonary granulocyte count is maximal [24]. Animals were imaged as described previously.

In vitro [125I]FIAU uptake in bacteria

Prior to its use for infection experiments *in vivo*, *E. coli RS218* was confirmed to be TK-positive through an *in vitro* [125I]FIAU uptake assay [20]. A known TK-negative strain, *E.coli KY895* [25], was used as the control. Overnight cultures of *E. coli RS218* (TK-positive) or *E. coli KY895 (*TK-negative) strains were diluted 1 in 50 in fresh Luria Bertani (LB) medium containing 1 μCi/mL (0.037 MBq/mL) of [125I]FIAU and incubated in a shaker incubator at 37°C for 2 to 24 h. At each specified time point, equal aliquots were withdrawn from the cultures and the cell pellets were washed three times to remove free [125I] FIAU in the media. The radioactivity in the pellets was measured using a gamma spectrometer (1282 Compugamma CS Universal gamma counter, LKB Wallac, Turku, Finland). Each assay was performed in triplicate.

Quantification of lung infection

E. coli RS218 was cultured to log phase in LB medium containing 100 μg/mL of streptomycin and was then serially diluted to provide different concentrations (colony forming units, CFU/mL) of infecting bacteria for mouse inoculation. Mice were anesthetized by isoflurane. Intranasal instillation of bacteria (10^5 – 10^7 CFU/mL) was performed in the anesthetized mice as described above. Infected mice were sacrificed at 18, 24 and 48 h after infection and their lungs were extracted and homogenized. Serial dilutions of the lung homogenate were plated onto blood TSA agar plates (Becton Dickinson, Franklin Lakes, NJ) for colony counting to estimate the bacterial load in the lung. Colony counting was performed at 24 h after plating.

SPECT-CT imaging of lung infection

Prior to infection, CD-1 mice were rendered neutropenic by intraperitoneal (i.p.) injection of cyclophosphamide (Baxter, Deerfield, IL) at day -4 (150 mg/kg) and at day -1 (100 mg/kg)[26]. Mice were injected *via* the tail vein with ~1 mCi (37 MBq) of [125I]FIAU and were imaged as described above at 2 – 8 h time points after injection of radiotracer, coinciding with 18 – 48 h after bacterial inoculation.

Image analysis

Signal intensity from SPECT images was calculated by using an automatic segmentation method we recently described [27]. Using standard image processing techniques, lungs of normal control and infected animals were presegmented from the CT. Typically, the infected regions of the lungs were omitted from this presegmentation followed by a template based deformation algorithm to complete the presegmentation. After segmentation of the lungs from the CT, the anatomic segmentation was superimposed upon the SPECT images and regions of interest (ROIs) were drawn. The average signal intensity within the lungs as well as the standard deviation of the [125I]FIAU-SPECT signal within the lungs was computed from the ROIs.

Histopathology

Infected or inflamed lungs were inflated and fixed in 10% neutral buffered formalin. Following fixation, specimens were placed into a tissue processing cassette and embedded in paraffin. Lungs were sectioned as 4 μm slices with a Reichert microtome, and stained with hematoxylin and eosin using standard methods.

Antibiotic treatment

Based on the results of a disk diffusion assay employing commonly used antibiotics [28], *E. coli RS218* was found to be susceptible to ampicillin and doxycycline, which were chosen for

treatment of lung infections in mice (data not shown). Antibiotic treatment was continued for 10 days at 50 mg/kg/day for ampicillin and 5 mg/kg/day for doxycycline as per dosage instructions on the package insert. Infected mice were imaged before and after treatment using the same parameters outlined above.

Ex vivo biodistribution

To measure the uptake of [125I]FIAU in mice with lung inflammation, mice were divided into two groups: PBS- (n = 8, control) and LPS-treated (n = 8). Four mice from each group were injected with 2 μCi (74 KBq) of [125I]FIAU in 200 μL of saline vehicle at 22 h after PBS or LPS treatment. The mice were then sacrificed at 24 h to determine the uptake of [125I]FIAU at 24 h after LPS administration. The remaining mice were injected with [125I]FIAU at 46 h and sacrificed at 48 h to determine the biodistribution at 48 h after LPS administration. For biodistribution experiments in infected mice, animals were infected intranasally with 10^5 - 10^7 CFU/mL of bacteria and then sacrificed at 18 - 48 h after infection. A separate group of mice that were infected with 10^5 CFU/mL bacteria were subsequently treated with antibiotics and used in the biodistribution study at the end of a 10 d treatment regimen. The organs that were collected for analysis included blood, heart, lungs, liver, spleen, kidney, stomach, small intestine and large intestine. The excised organs were weighed and counted in a gamma counter and the percentage injected dose per gram (%ID/g) of organ was calculated from the data.

Statistical analysis

In comparisons of *ex vivo* biodistribution studies and image analysis data among the inflamed, infected and treated groups, statistical analyses were performed using a one way ANOVA. To compare between the LPS- and PBS-treated mice, a two-tailed t test was used. In all analyses, *P*-values less than 0.05 were considered significant. All analyses were performed using Prism software (GraphPad Software, La Jolla, CA).

Results

Validation of the inflammation model

The time point at which there was maximum inflammation, as evidenced by the total cell counts within lung, was at 24 h following the intranasal administration of LPS (**Figure 1**). At that time the total granulocyte count was (2.60 ± 0.15) x 10^6 cells. Thereafter, a steady decline in the total cell numbers reaching (0.80 ± 0.31) x 10^6 cells by 48 h was observed (**Table 1**). The calculated granulocyte cell numbers in the control mice averaged over 48 h were (0.25 ± 0.19) x 10^6 cells. Accordingly, the 24 h time point was chosen for subsequent imaging experiments. The calculated lung weights show an increase in weight of the LPS mice lungs in the range of 14 – 25% over the control, which is consistent with values reported in the literature [24].

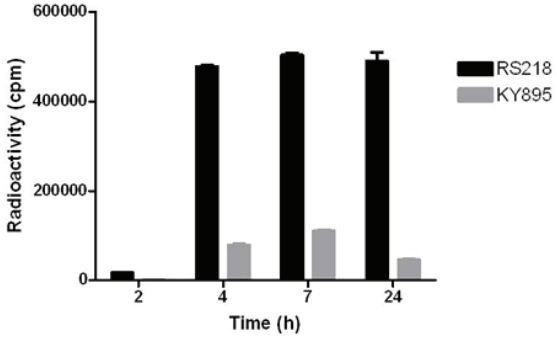

Figure 1. [125I]FIAU cell uptake specificity. *E. coli RS218* and *E. coli KY895* were incubated with 1 μCi/mL (37 MBq/mL) [125I]FIAU in an incubator at 37°C. Accumulated radioactivity was measured by withdrawing equal aliquots of *E. coli RS218* (black bars) and *E. coli KY895* (gray bars) at different time points (2 h – 24 h) following incubation with radiotracer. Values depicted are the average from three aliquots of experiments performed in triplicate. Data are represented as accumulated activity in counts per minute (cpm) ± SEM.

Table 1. Time course of lung granulocyte accumulation after LPS treatment

Time (h)	*Total Granulocytes per mL (x 10^6)*
PBS	0.25 ± 0.19
0	0.67 ± 0.06
12	1.59 ± 0.33
24	2.60 ± 0.15
36	1.26 ± 0.36
48	0.80 ± 0.31

Ex vivo biodistribution

The biodistribution values in the lungs showed no difference in uptake between the controls (1.26 ± 0.27 %ID/g) and LPS-treated mice (1.69 ± 0.40 %ID/g) (*P* = 0.18) (**Table 2**, **Figure 2**). As

Table 2. *Ex vivo* biodistribution – inflamed lungs (% ID/g ± SEM , n = 4)

Organ	*PBS (24 h)*	*LPS (24 h)*	*PBS (48 h)*	*LPS (48 h)*
blood	1.82 ± 0.46	2.28 ± 0.70	1.57 ± 0.46	2.12 ± 0.68
heart	0.75 ± 0.11	1.04 ± 0.09	0.34 ± 0.11	0.59 ± 0.29
lung	1.26 ± 0.27	1.69 ± 0.40	0.91 ± 0.32	0.90 ± 0.54
liver	0.93 ± 0.15	1.39 ± 0.11	0.56 ± 0.21	0.73 ± 0.19
stomach	7.13 ± 2.01	9.02 ± 3.99	4.30 ± 2.21	4.37 ± 3.18
spleen	0.82 ± 0.62	1.64 ± 0.37	0.88 ± 0.33	1.21 ± 0.43
kidney	1.88 ± 0.27	2.89 ± 0.95	0.99 ± 0.33	1.41 ± 0.50
muscle	0.40 ± 0.03	0.59 ± 0.11	0.02 ± 0.00	0.01 ± 0.00
small int.	2.04 ± 0.26	1.78 ± 0.59	1.00 ± 0.41	1.44 ± 0.46

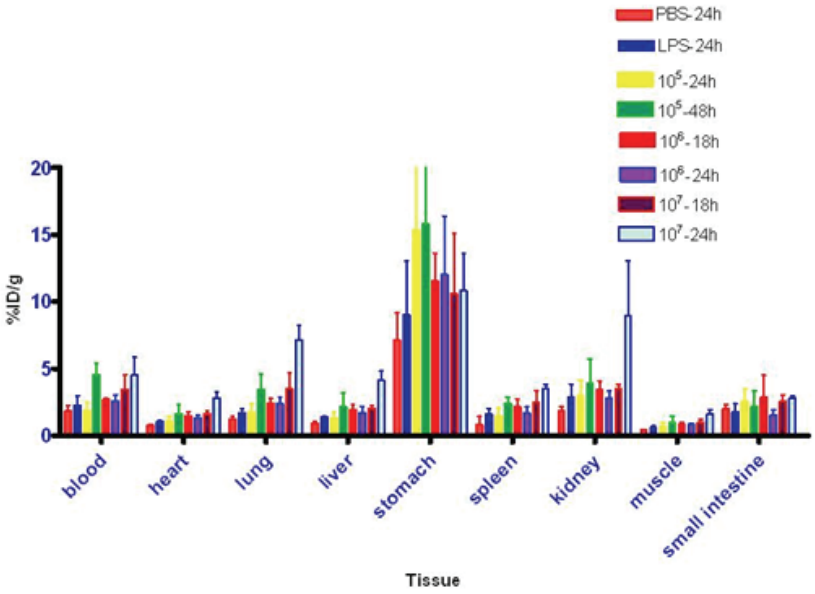

Figure 2. *Ex vivo biodistribution data in lung inflammation and infection.* Control mice, mice treated with lipopolysaccharide (LPS, an inducer of inflammation) and mice that were infected with different bacterial concentrations (10^5 to 10^7 CFU/mL) were injected with 2 μCi (74 KBq) [125I]FIAU *via* the tail vein. At 2 h following injection of radiotracer, and coinciding with 18 h, 24 h or 48 h following administration of phosphate-buffered saline (PBS), LPS or bacteria, mice were sacrificed and their organs were harvested, weighed and radioactivity was counted in a gamma spectrometer. Values are represented as percentage of injected dose (%ID) per gram of tissue. Data are means ± SEM of four animals.

Table 3. *Ex vivo* biodistribution – infected lungs (% ID/g ± SEM , n = 3)

	10^7-24hr	*10^7-18hr*	*10^6-24hr*	*10^6-18hr*	*10^5-48hr*	*10^5-24hr*
blood	4.52 ± 1.32	3.45 ± 1.09	2.60 ± 0.45	2.69 ± 0.07	4.53 ± 0.88	1.88 ± 0.58
heart	2.80 ± 0.47	1.59 ± 0.23	1.28 ± 0.23	1.47 ± 0.32	1.33 ± 0.72	1.06 ± 0.36
lung	7.14 ± 1.09	3.50 ± 1.20	2.36 ± 0.54	2.42 ± 0.34	3.43 ± 1.69	1.68 ± 0.75
liver	4.10 ± 0.72	2.03 ± 0.19	1.73 ± 0.46	1.93 ± 0.41	2.14 ± 1.02	1.33 ± 0.44
stomach	10.81 ± 2.80	10.62 ± 4.47	12.02 ± 4.36	11.57 ± 2.04	15.81 ± 7.97	15.31 ± 10.10
spleen	3.48 ± 0.34	2.48 ± 0.90	1.69 ± 0.46	2.19 ± 0.56	2.36 ± 0.51	1.43 ± 0.63
kidney	8.97 ± 4.06	3.51 ± 0.33	2.80 ± 0.52	3.42 ± 0.66	3.87 ± 1.85	2.94 ± 1.20
muscle	1.65 ± 0.25	1.00 ± 0.19	0.86 ± 0.05	0.84 ± 0.14	0.75 ± 0.12	0.68 ± 0.28
small int.	2.79 ± 0.18	2.53 ± 0.54	1.55 ± 0.38	2.85 ± 1.65	2.18 ± 1.17	2.54 ± 0.94

expected, high radiochemical uptake was also detected in the stomach, liver and intestines [18, 29]. Bacterial infection in lungs showed uptake values of 7.14 ± 1.09 for the highest level of infection (24 h following infection with 10^7 CFU/mL) down to 1.68 ± 0.75 %ID/g for the lowest infection dose (24 h following infection with 10^5 CFU/mL) (**Table 3, Figure 2**). Lung uptake values reduced to 1.78 ± 0.50 %ID/g from 3.43 ± 1.69 %ID/g (48 h following infection with 10^5 CFU/mL) after antibiotic (doxycycline) treatment ($P < 0.05$) (**Table 4**, **Figure 3**). The *P*-value

Table 4. *Ex vivo* biodistribution – antibiotic treatment (% ID/g ± SEM, n = 4)

	No treatment	*Ampicillin*	*Doxycycline*
blood	4.53 ± 0.88	3.06 ± 0.74	3.35 ± 0.95
heart	1.33 ± 0.72	1.24 ± 0.09	1.16 ± 0.21
lung	3.43 ± 1.69	2.05 ± 0.33	1.78 ± 0.50
liver	2.14 ± 1.02	1.60 ± 0.13	1.43 ± 0.30
stomach	15.81 ± 7.97	11.16 ± 6.21	7.57 ± 2.64
spleen	2.36 ± 0.51	1.73 ± 0.24	2.39 ± 1.21
kidney	3.87 ± 1.85	3.45 ± 0.15	3.59 ± 0.45
muscle	0.75 ± 0.12	0.78 ± 0.06	0.71 ± 0.18
small int.	2.18 ± 1.17	2.16 ± 0.49	1.72 ± 0.46

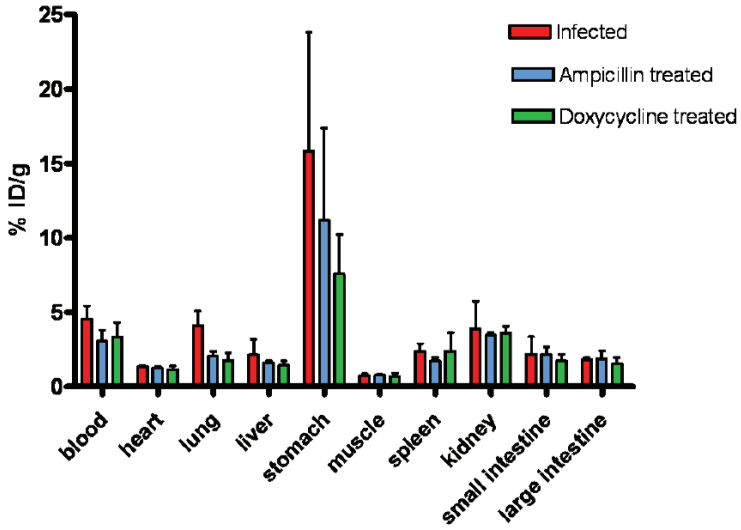

Figure 3. *Ex vivo* biodistribution data for [125I]FIAU uptake in infected and antibiotic treated animals. Mice infected with 10^5 CFU/mL *E. coli RS218* at 48 h after infection were used as the infected group. Mice that were infected with 10^5 CFU/mL *E. coli RS218* and subsequently administered antibiotics beginning at 48 h after infection represent the treatment group. Both groups received 2 μCi (74 KBq) [125I]FIAU *via* the tail vein and were sacrificed at 2 h following radiotracer injection. Organs were harvested, weighed and radioactivity was counted in a gamma spectrometer. Values are represented as percentage of injected dose (%ID) per gram of tissue. Data are means ± SEM of five animals.

of a one-way ANOVA used for comparison among the different degrees of infection was less than 0.0001. Ampicillin treatment led to a decrease in radiochemical uptake as well, to 2.05 ± 0.30 %ID/g. High blood uptake values were seen in infected mice that trended toward decrease in treated animals.

Imaging of lung inflammation and infection

Animals with lung inflammation or infection were imaged at 2 h following intravenous (i.v.) injection of [125I]FIAU. **Figures 4A** and **B** show the SPECT-CT images of mice scanned at 24 h after administration of PBS or LPS. Images were adjusted to the same threshold intensity. No detectable signal was visible in mouse lungs that were inflamed (**Figure 4B**). The mean lung uptake values extracted from the images were 2.78 ± 0.87 and 2.10 ± 0.70 for the PBS- and LPS-treated mice, respectively ($P = 0.09$). Based on these results we conclude that sterile inflammation does not sequester [125I]FIAU.

Bacterial infection in mouse lungs showed selective uptake of [125I]FIAU. Animals that were infected with 10^5 CFU/mL *E. coli RS218* could be visualized in the lungs at 48 h after infection when the bacterial burden was (5.9 ± 0.8) x 10^{11} CFU/mL, as measured from *ex vivo* bacterial culture, i.e., bacterial quantification obtained from culture of the mouse lungs (**Table 5**). For the same infecting dose, the bacteria could not be visualized at 24 h following infection when the bacterial burden in the lungs was only (3.5 ± 1.4) x 10^7 CFU/mL. For mice that were infected with 10^6 CFU/mL, the bacterial burden was (3.6 ± 2.4) x 10^9 CFU/mL and (1.4 ± 0.4) x 10^9 CFU/mL at 18 and 24 h after infection, respectively. For animals that were in-

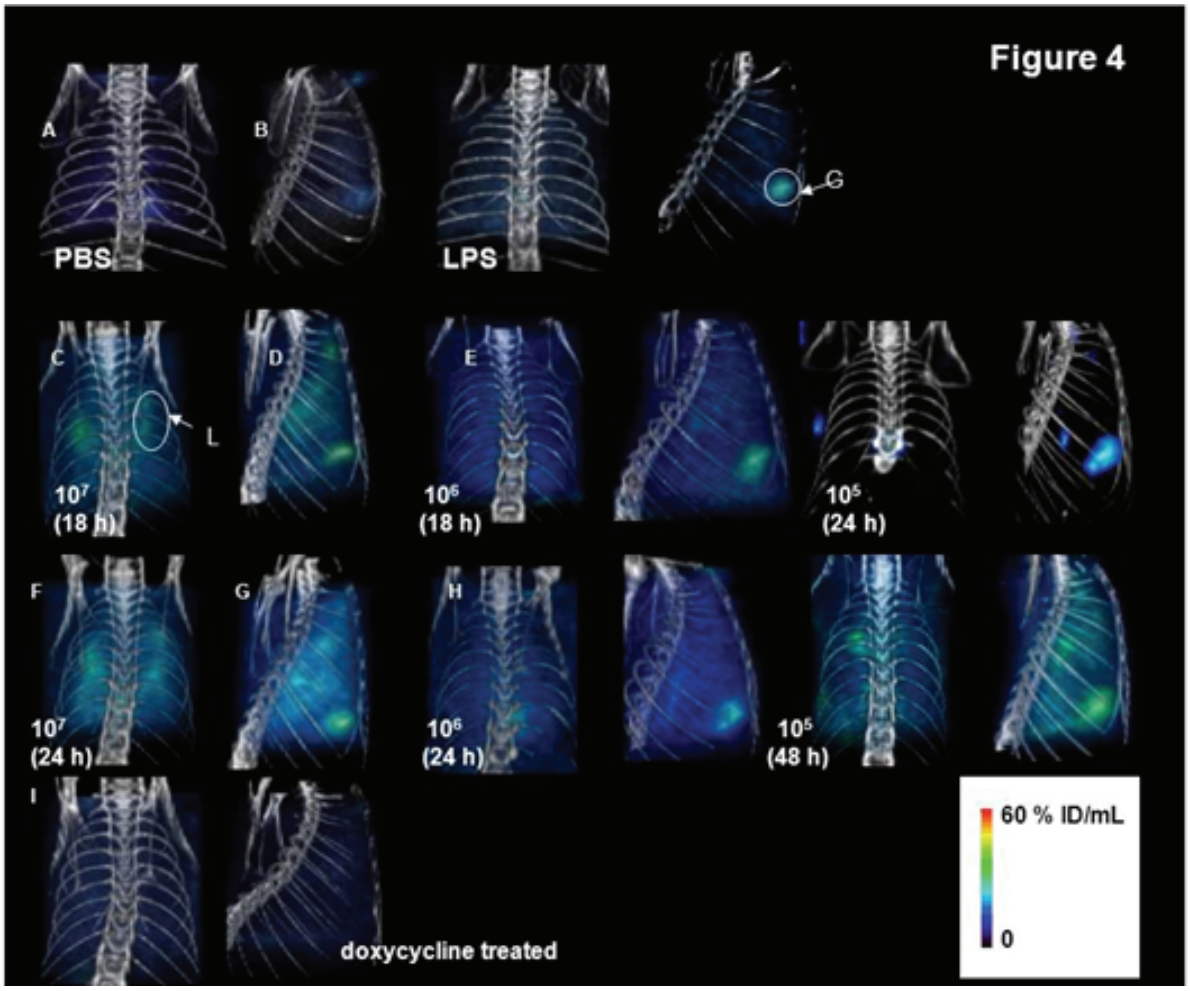

Figure 4. SPECT-CT imaging of lung inflammation and infection. Control (PBS) and LPS-treated (inflammation) mice were injected with 1 mCi (37 MBq) of [125I]FIAU *via* the tail vein and SPECT-CT images were acquired at (A) 24 h after PBS administration (control), (B) 24 h after LPS administration. Four mice were imaged per group. All scans were performed two hours after injection of [125I]FIAU. All images were adjusted to the same maximum signal threshold. Mice harboring lung infection were similarly injected with 1 mCi (37 MBq) of [125I]FIAU with SPECT-CT images acquired at 18 h after infection with (C)10^7 CFU/mL, (D) 10^6 CFU/mL, and at 24 h after infection with (E) 10^5 CFU/mL of *E. coli RS218*. SPECT-CT images of mice imaged at 24 h after infection with (F) 10^7 CFU/mL, (G) 10^6 CFU/mL and at 48 h after infection with (H) 10^5 CFU/mL of *E. coli RS218*. Four mice were imaged for each bacterial infecting dose. For monitoring antibiotic therapy, SPECT-CT images (I) of a mouse inoculated with 10^5 CFU/mL *E. coli RS218* and with doxycycline for 10 days (5 mg/kg/day) were obtained. Four mice were imaged per group. A representative image is depicted for each group. G – gallbladder, S- stomach, L- Lung.

fected with 10^7 CFU/mL of bacteria, the bacterial load in the lungs was (1.6 ± 0.1) x 10^{12} CFU/mL at 18 h following infection. At lung bacterial concentrations of 10^9 – 10^{12} CFU/mL, bacteria could be visualized on the SPECT scan as a diffuse signal in the lungs (**Figures 4C** – **H**). Infection in animals that were infected with higher CFU/mL bacteria could be visualized at the earlier time point of 18 h. Although we imaged mice at later time points and following inoculation with 10^8 CFU/mL, we did not ascertain the bacterial burden in the lungs of these animals. Decreased bacteria were seen in the lungs upon treatment with antibiotics (compare **Figure 4H** to **I**, the latter obtained after treatment with doxycycline).

Image analysis

For each animal we computed the average

Table 5. Lung bacterial load and signal intensity calculated from SPECT-CT images

Infection dose-(CFU/mL)	*Time after infection (h)*	*CFU/mL*	Average Image Intensity (AV) ± SEM (%ID/mL)
10^5	24	$(3.5 \pm 1.4) \times 10^7$	11.21 ± 5.37
10^5	48	$(5.9 \pm 0.8) \times 10^{11}$	29.21 ± 10.64
10^6	18	$(3.6 \pm 2.4) \times 10^9$	17.32 ± 6.44
10^6	24	$(1.4 \pm 0.38) \times 10^9$	8.90 ± 5.26
10^7	18	$(1.6 \pm 0.05) \times 10^{12}$	30.37 ± 4.03
10^7	24	not determined	24.03 ± 0.61
LPS	24	n/a	2.10 ± 0.00
PBS-control	24	n/a	2.78 ± 0.00

value (AV) of the [125I]FIAU uptake on the SPECT image within the ROI corresponding to the lungs. The results are presented in **Table 5**. The regression of log AV onto log CFU is presented in **Figure 5**, providing a standard curve, enabling us to read the number of bacteria in the lungs directly from the image. The correlation between image intensity and number of bacteria present within the lungs is significant (*P*-value < 10^{-5}) for both the Pearson (Pearson, R = 0.78) and Spearman correlation tests.

Histopathology

Compared to control lungs (**Figure 6A**), mouse lungs that were inflamed by LPS treatment (**Figure 6B**) showed a predominance of neutrophils due to the inflammatory response arising from the insult. **Figures 6C** and **6D** demonstrate the presence of bacteria inside alveoli after inoculation of *E. coli*.

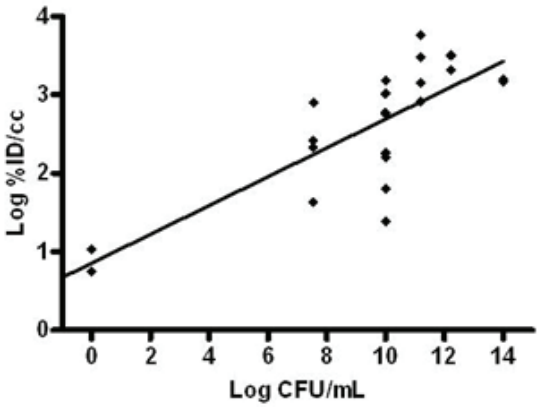

Figure 5. Average Value (AV) of [125I]FIAU SPECT signal intensity within the region-of-interest corresponding to the lungs *versus* colony forming units per mL (CFU/mL) in log scale together with the line of regression (Pearson R = 0.78).

Discussion

Radiolabeled analogs of FIAU have been used to image bacterial infection in experimental models and in human subjects previously [18, 19]. Due to the presence of sequence homology within the consensus catalytic domain of TK in several different bacterial strains, most bacteria and mycoplasma are able to metabolize FIAU. However, the consensus sequence does not exist in mammalian TKs, which explains the poor capability of mammalian cells to metabolize FIAU. We undertook the current study with two goals in mind: 1) to validate the method, i.e., determine whether or not [125I]FIAU was specific for infection, or could also image sterile inflammation; and, 2) to estimate the sensitivity of detection of this radiopharmaceutical-based technique and define whether it could be used effectively in longitudinal murine infection models to test new antibiotics. We demonstrate using SPECT-CT that [125I]FIAU indeed does not show specific uptake in sterile inflammation, corroborating earlier experiments that employed this tracer in *ex vivo* studies performed in rats [30]. In contrast to earlier studies in which [125I]FIAU was used to image localized bacterial infection [18] or caseous lesions within the lungs caused by *M. tuberculosis* [20], the method of bacterial infection by the intranasal route employed in this study resulted in infections that assume a more diffuse pattern within the lungs. Although in the present study we used [125I]FIAU, using positron-emitting analogs of FIAU combined with positron emission tomography (PET) would enable higher sensitivity (5 – 50 fold) [31], which would enable imaging of fewer bacteria. Despite the diffuse pattern of the infection and the use of a low-energy radionuclide

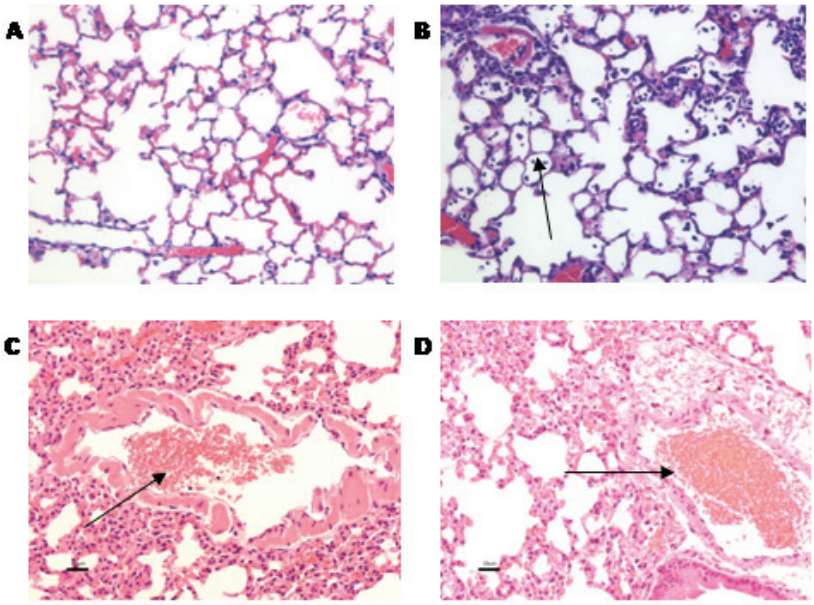

Figure 6. Mouse lung histology. Histological staining with hematoxylin and eosin (H & E) of mouse lungs. (A) PBS-treated (control); (B) LPS-treated (inflamed); (C) bacterial infection at 48 h after inoculation with 10^5 CFU/mL bacteria; (D) bacterial infection at 18 h after inoculation with 10^7 CFU/mL bacteria. Arrows depict the presence of neutrophils (A, B) and bacterial colonies (C, D) inside the alveoli.

not optimized for imaging ([^{125}I]FIAU), we showed that we were able to detect and image lung infection following inoculation with TK-positive *E. coli*. The level of detection that can be visualized in a SPECT scan corresponded to a bacterial concentration in the lungs of 10^9 CFU/mL. In spite of the fact that the %ID per mL within the lungs is significantly higher than the controls at a much lower bacterial load, we define the level of detection when a distinct signal can be visualized over the lungs, and this corresponds to 10^9 CFU/mL. Although the number of bacteria present on the image to allow visual detection is several orders of magnitude higher than for fluorescent probes [32-34] and bioluminescence (~ 10^6 CFU/lung), bioluminescence requires genetic manipulation of the cells (introduction of a luciferase) [35], administration of large amounts of luciferin (on the order of 100 mg/kg), and is not readily amenable to quantification due to the attenuation of signal through the tissues. Furthermore, in contrast to bioluminescence, SPECT or PET imaging using radiolabeled versions of FIAU is directly translatable to human applications, and therefore of critical importance for establishing the link between antibiotics investigated in preclinical models and in patients.

We also applied FIAU imaging methodology to monitor a course of routinely used antibiotics. We were able to show decreased lung signal in infected animals over time with treatment that achieved significance in the case of doxycycline and approached significance for ampicillin. Imaging eliminates the need for time-consuming and invasive methods that require collection and culture of specimens that are currently in use. Moreover, since this method is noninvasive, fewer animals can be imaged repeatedly, serving as their own controls, enabling a more statistically robust study. FIAU at high concentrations (> 32 μg/mL) is known to inhibit the growth of bacteria that have endogenous TK [18]. In our current experiments, the standard dose of [^{125}I]FIAU per animal of 2 – 5 mCi (74 – 185 MBq) is equivalent to 0.34 – 0.85 μg of FIAU per animal, far below the pharmacologic dose.

Radiolabeled FIAU satisfies most criteria for functioning as an effective radiopharmaceutical for imaging infection. Radiolabeled FIAU demonstrates rapid accumulation at specific sites of infection – even if those infections are diffuse, such as within the lungs, rather than being focal, such as with an abscess – with low uptake in uninfected regions. It is nontoxic, safe and easy to prepare. Above all, it demonstrates the ability to differentiate between infection and sterile inflammation, and compares favorably in this regard with [^{18}F]fluorodeoxyglucose and other agents being considered for imaging infection. We have also shown that it can be used, in principle, to follow antibiotic treatment in a preclinical model of infection, although the sensitiv-

ity of detection is lower than for optically-based techniques.

Acknowledgments

We would like to thank Dr. Kwang Sik Kim for providing us with *E. coli RS218* and the Coli Genetic Stock Center (CGSC) at Yale University for providing us with the bacterial strain *E. coli KY895*. We thank Drs. Sridhar Nimmagadda and Catherine Foss for helpful discussions and for critical reading of the manuscript and Dr. Sanjay Jain for helpful discussions. We also thank Gilbert Green for help with SPECT-CT imaging and Dr. David Huso for help with histology. The work was supported by AstraZeneca Discovery Medicine, NIH U24 CA92871 and R01 EB009367.

Address correspondence to: Dr. Martin G Pomper, Johns Hopkins Medical Institutions, 1550 Orleans Street, 492 CRB II, Baltimore, MD 21231 Tel: 410-955-2789; Fax: 443-817-0990; E-mail: mpomper@jhmi.edu

References

[1] Jarvis WR. Prevention and control of methicillin-resistant Staphylococcus aureus: dealing with reality, resistance, and resistance to reality. Clin Infect Dis 2010; 50: 218-220.

[2] Subha A and Ananthan S. Extended spectrum beta lactamase (ESBL) mediated resistance to third generation cephalosporins among Klebsiella pneumoniae in Chennai. Indian J Med Microbiol 2002; 20: 92-95.

[3] Samonis G and Bafaloukos D. Fungal infections in cancer patients: an escalating problem. In Vivo 1992; 6: 183-193.

[4] Gasink LB and Blumberg EA. Bacterial and mycobacterial pneumonia in transplant recipients. Clin Chest Med 2005; 26: 647-659, vii.

[5] Vinh DC and Embil JM. Device-related infections: a review. J Long Term Eff Med Implants 2005; 15: 467-488.

[6] El-Haddad G, Zhuang H, Gupta N and Alavi A. Evolving role of positron emission tomography in the management of patients with inflammatory and other benign disorders. Semin Nucl Med 2004; 34: 313-329.

[7] Tahara T, Ichiya Y, Kuwabara Y, Otsuka M, Miyake Y, Gunasekera R and Masuda K. High [18F]-fluorodeoxyglucose uptake in abdominal abscesses: a PET study. J Comput Assist Tomogr 1989; 13: 829-831.

[8] Ascher NL, Ahrenholz DH, Simmons RL, Weiblen B, Gomez L, Forstrom LA, Frick MP, Henke C and McCullough J. Indium 111 autologous tagged leukocytes in the diagnosis of intraperitoneal sepsis. Arch Surg 1979; 114: 386-392.

[9] Beckers C, Jeukens X, Ribbens C, Andre B, Marcelis S, Leclercq P, Kaiser MJ, Foidart J, Hustinx R and Malaise MG. (18)F-FDG PET imaging of rheumatoid knee synovitis correlates with dynamic magnetic resonance and sonographic assessments as well as with the serum level of metalloproteinase-3. Eur J Nucl Med Mol Imaging 2006; 33: 275-280.

[10] Fernandez-Ulloa M, Hughes JA, Krugh KB and Chin D. Bone imaging in infections: artefacts from spectral overlap between a Tc-99m tracer and In-111 leukocytes. J Nucl Med 1983; 24: 589-592.

[11] Thakur ML, Lavender JP, Arnot RN, Silvester DJ and Segal AW. Indium-111-labeled autologous leukocytes in man. J Nucl Med 1977; 18: 1014-1021.

[12] Welling MM, Lupetti A, Balter HS, Lanzzeri S, Souto B, Rey AM, Savio EO, Paulusma-Annema A, Pauwels EK and Nibbering PH. 99mTc-labeled antimicrobial peptides for detection of bacterial and Candida albicans infections. J Nucl Med 2001; 42: 788-794.

[13] Benitez A, Roca M and Martin-Comin J. Labeling of antibiotics for infection diagnosis. Q J Nucl Med Mol Imaging 2006; 50: 147-152.

[14] Edwards DS, Liu S, Ziegler MC, Harris AR, Crocker AC, Heminway SJ, Barrett JA, Bridger GJ, Abrams MJ and Higgins JD 3rd. RP463: a stabilized technetium-99m complex of a hydrazino nicotinamide derivatized chemotactic peptide for infection imaging. Bioconjug Chem 1999; 10: 884-891.

[15] Becker W and Meller J. The role of nuclear medicine in infection and inflammation. Lancet Infect Dis 2001; 1: 326-333.

[16] Rennen HJ, Boerman OC, Oyen WJ and Corstens FH. Imaging infection/inflammation in the new millennium. Eur J Nucl Med 2001; 28: 241-252.

[17] Bleeker-Rovers CP, Boerman OC, Rennen HJ, Corstens FH and Oyen WJ. Radiolabeled compounds in diagnosis of infectious and inflammatory disease. Curr Pharm Des 2004; 10: 2935-2950.

[18] Bettegowda C, Foss CA, Cheong I, Wang Y, Diaz L, Agrawal N, Fox J, Dick J, Dang LH, Zhou S, Kinzler KW, Vogelstein B and Pomper MG. Imaging bacterial infections with radiolabeled 1-(2'-deoxy-2'-fluoro-beta-D-arabinofuranosyl)-5-iodouracil. Proc Natl Acad Sci USA 2005; 102: 1145-1150.

[19] Diaz LA Jr, Foss CA, Thornton K, Nimmagadda S, Endres CJ, Uzuner O, Seyler TM, Ulrich SD, Conway J, Bettegowda C, Agrawal N, Cheong I, Zhang X, Ladenson PW, Vogelstein BN, Mont MA, Zhou S, Kinzler KW, Vogelstein B and Pomper MG. Imaging of musculoskeletal bacterial infections by [124I]FIAU-PET/CT. PLoS One 2007; 2: e1007.

[20] Davis SL, Be NA, Lamichhane G, Nimmagadda S, Pomper MG, Bishai WR and Jain SK. Bacterial thymidine kinase as a non-invasive imaging reporter for Mycobacterium tuberculosis in live animals. PLoS One 2009; 4: e6297.
[21] Brader P, Stritzker J, Riedl CC, Zanzonico P, Cai S, Burnazi EM, Ghani ER, Hricak H, Szalay AA, Fong Y and Blasberg R. Escherichia coli Nissle 1917 facilitates tumor detection by positron emission tomography and optical imaging. Clin Cancer Res 2008; 14: 2295-2302.
[22] Jacobs A, Braunlich I, Graf R, Lercher M, Sakaki T, Voges J, Hesselmann V, Brandau W, Wienhard K and Heiss WD. Quantitative kinetics of [124I]FIAU in cat and man. J Nucl Med 2001; 42: 467-475.
[23] Chignard M and Balloy V. Neutrophil recruitment and increased permeability during acute lung injury induced by lipopolysaccharide. Am J Physiol Lung Cell Mol Physiol 2000; 279: L1083-1090.
[24] Szarka RJ, Wang N, Gordon L, Nation PN and Smith RH. A murine model of pulmonary damage induced by lipopolysaccharide via intranasal instillation. J Immunol Methods 1997; 202: 49-57.
[25] Kit S, Otsuka H, Qavi H and Hazen M. Herpes simplex virus thymidine kinase activity of thymidine kinase-deficient Escherichia coli K-12 mutant transformed by hybrid plasmids. Proc Natl Acad Sci USA 1981; 78: 582-586.
[26] Zuluaga AF, Salazar BE, Rodriguez CA, Zapata AX, Agudelo M and Vesga O. Neutropenia induced in outbred mice by a simplified low-dose cyclophosphamide regimen: characterization and applicability to diverse experimental models of infectious diseases. BMC Infect Dis 2006; 6: 55.
[27] Vidal C HJ, Davis S, Younes L, Jain S, Jedynak B. Template Registration with Missing Parts: Application to the Segmentation of Tuberculosis Infected Lungs. Paper presented at: SPIE Proceedings of the International Symposium on Biomedical Images 2009, Boston, MA.
[28] Ubukata K, Chiba N, Hasegawa K, Shibasaki Y, Sunakawa K, Nonoyama M, Iwata S and Konno M. Differentiation of beta-lactamase-negative ampicillin-resistant Haemophilus influenzae from other H. influenzae strains by a disc method. J Infect Chemother 2002; 8: 50-58.
[29] Morgenroth A, Deisenhofer S, Neininger M, Vogg AT, Glatting G, Kull T and Reske SN. Biodistribution, cellular uptake and DNA-incorporation of the 2'-fluoro stabilized 5-iodo-2'-deoxyuridine analog 5-iodo-(2-deoxy-2-fluoro-beta-D-arabinofuranosyl)uracil (FIAU). Q J Nucl Med Mol Imaging 2008; 52: 305-316.
[30] Laverman P, Corstens FHM, Oyen WJG and Boerman OC. Radiolabeled FIAU can discriminate between bacterial infection and sterile inflammation. Eur J Nucl Med Mol Imaging 2007; 34: S397-S397.
[31] Tjuvajev JG, Finn R, Watanabe K, Joshi R, Oku T, Kennedy J, Beattie B, Koutcher J, Larson S and Blasberg RG. Noninvasive imaging of herpes virus thymidine kinase gene transfer and expression: a potential method for monitoring clinical gene therapy. Cancer Res 1996; 56: 4087-4095.
[32] Petruzzi N, Shanthly N and Thakur M. Recent trends in soft-tissue infection imaging. Semin Nucl Med 2009; 39: 115-123.
[33] Leevy WM, Gammon ST, Jiang H, Johnson JR, Maxwell DJ, Jackson EN, Marquez M, Piwnica-Worms D and Smith BD. Optical imaging of bacterial infection in living mice using a fluorescent near-infrared molecular probe. J Am Chem Soc 2006; 128: 16476-16477.
[34] Leevy WM, Gammon ST, Johnson JR, Lampkins AJ, Jiang H, Marquez M, Piwnica-Worms D, Suckow MA and Smith BD. Noninvasive optical imaging of staphylococcus aureus bacterial infection in living mice using a Bis-dipicolylamine-Zinc(II) affinity group conjugated to a near-infrared fluorophore. Bioconjug Chem 2008; 19: 686-692.
[35] Rocchetta HL, Boylan CJ, Foley JW, Iversen PW, LeTourneau DL, McMillian CL, Contag PR, Jenkins DE and Parr TR Jr. Validation of a noninvasive, real-time imaging technology using bioluminescent Escherichia coli in the neutropenic mouse thigh model of infection. Antimicrob Agents Chemother 2001; 45: 129-137.